Biomaterials 30 (2009) 1532–1541

Contents lists available at ScienceDirect

Biomaterials

journal homepage: www.elsevier.com/locate/biomaterials

The effect of 3-hydroxybutyrate methyl ester on learning and memory in mice

Xiang-Hui Zou [a,b], Hong-Ming Li [a], Sheng Wang [c], Michael Leski [d], Yong-Chao Yao [a], Xiao-Di Yang [a], Qing-Jun Huang [c], Guo-Qiang Chen [a,e,*]

[a] Multidisciplinary Research Center, Shantou University, Shantou 515063, Guangdong, China
[b] Department of Biology, Hanshan Normal University, Chaozhou, Guangdong, 521041, China
[c] Mental Health Center, Shantou University, Shantou 515063, Guangdong, China
[d] Advanced Life Sciences, Woodridge, IL 60517, USA
[e] Department of Biological Science and Biotechnology, Tsinghua University, Beijing 100084, China

ARTICLE INFO

Article history:
Received 17 October 2008
Accepted 4 December 2008
Available online 27 December 2008

Keywords:
PHB
3-Hydroxybutyrate methyl ester
Learning and memory
PUMA-G
Connexin
Gap junctional intercellular communication

ABSTRACT

Learning and memory requires energy-demanding cellular processes and can be enhanced when the brain is supplemented with metabolic substrates. In this study, we found that neuroglial cell metabolic activity was significantly elevated when cultured in the presence of polyhydroxybutyrate (PHB) degradation product 3-hydroxybutyrate (3-HB) and derivatives. We demonstrated that the receptor for 3-HB, namely, protein upregulated in macrophages by IFN-γ (PUMA-G), was expressed in brain and upregulated in mice treated with 3-hydroxybutyrate methyl ester (3-HBME). We also affirmed increased expression of connexin 36 protein and phosphorylated ERK2 (extracellular signal-regulated kinase 2) in brain tissues following 3-HBME treatment, although these differences were not statistically significant. Mice treated with 3-HBME performed significantly ($p < 0.05$) better in the Morris water maze than either the negative controls (no treatment) or positive controls (acetyl-L-carnitine treatment). Moreover, we found that 3-HBME enhanced gap junctional intercellular communication between neurons. Thus, 3-HB and derivatives enhance learning and memory, possibly through a signaling pathway requiring PUMA-G that increases protein synthesis and gap junctional intercellular communication.

1. Introduction

Memory formation after a learning experience correlates with increases in synaptic transmission and morphological alterations at the synapse, both of which add to the energetic workload of the neuron. Distinct areas of the hippocampus are metabolically active at different times during spatial learning tasks, supporting the involvement of a type of metabolic plasticity involving neuron–glia coupling [1,2]. Astrocytes couple synaptic activity to glucose consumption through molecular mechanisms that involve the sequential intervention of astrocyte-specific glutamate transporters and the sodium–potassium ATPase, activation of glycolysis in astrocytes, and monocarboxylate transporter-mediated exchange of lactate from astrocytes to neurons [3–5].

The monocarboxylate transporter also transports ketone bodies including 3-HB. Ketone bodies are normally produced by the liver from fatty acids and released into the vasculature as an energy source for extra hepatic tissues, especially during starvation or disease [6]. 3-HB is the most common degradation product of microbial polyhydroxybutyrate (PHB) that has been investigated for tissue engineering application [7]. Evidence has been accumulated for a therapeutic role of ketone bodies in neuronal disorders. For example, 3-HB conferred partial protection to hippocampal neurons against beta-amyloid 1–42 toxicity, and preserved neuronal integrity and stability during glucose deprivation [8,9]. Alzheimer's disease and many other multifactorial cognitive or neurological disorders are rapidly growing public health concerns with potentially devastating effects [10,11]. Although numerous studies have described either the etiology of these diseases or compounds that protect neurons, an effective therapy is yet to be developed [12,13].

We previously reported that 3-HB enabled cultured cells to reach high confluencies by preventing cell death [14]. We speculated that 3-HB was converted to acetyl-CoA, which would support a greater mitochondrial membrane potential ($\Delta\psi_m$) and in turn prevent cell death. Subsequently, 3-HB was proposed as the endogenous ligand for PUMA-G [15], a G-protein-coupled receptor expressed in adipose tissue. This supports the alternative explanation that 3-HB protects cells through a signaling pathway activated by this receptor, although PUMA-G was reported to have a limited tissue distribution that did not include the brain [16]. Additionally, our previous observation that 3-HB was most effective at high confluencies hints

* Corresponding author. Multidisciplinary Research Center, Shantou University, Shantou 515063, Guangdong, China. Tel.: +86 754 82901186; fax: +86 754 82901175.
E-mail address: chengq@stu.edu.cn (G.-Q. Chen).

0142-9612/$ – see front matter © 2008 Elsevier Ltd. All rights reserved.
doi:10.1016/j.biomaterials.2008.12.012

that functional gap junctions promote cell survival, so the possibility that gap junctional intercellular communication is upregulated under these conditions must be considered. Interestingly, neuronal gap junctions incorporating connexin 36 play a role in learning and memory [17]. Thus, the possibility that 3-HB may foster learning and memory must also be considered.

Many researches focus on the applications of polyhydroxyalkanoates (PHA) as implant biomaterials, and found that PHA has good biocompatibility and biodegradability [18–20]. In vivo, PHB degradation products 3-HB or derivatives may enter the brain through the blood–brain barrier and then produce some effects. This study sought to investigate the effect of 3-HB and derivatives on neuroglial cell metabolic activity and gap junctional intercellular communication of hippocampal neurons, to evaluate the hippocampal expression of PUMA-G and proteins related to memory following treatment with 3-HB, and to determine whether 3-hydroxybutyrate methyl ester (3-HBME) improves learning and memory in the normal mouse.

2. Materials and methods

2.1. Materials

BALB/c mice were purchased from Shanghai Slac Laboratory Animal Co. Ltd. (Shanghai, China). Polyhydroxybutyrate (PHB) was kindly donated from Microbiology Laboratory, Tsinghua University (Beijing, China). 3-HB, B27 additives, 6-CFDA and 3-(4,5-dimethylthiazol-2-yl)-2,5-diphenyl tetrazolium bromide (MTT) were purchased from Sigma Chemical Co. (USA). Penicillin–streptomycin, trypsinase were purchased from Guangzhou Whiga Technology Co. Ltd. (China). Fetal Bovine Serum (FBS) (HyClone, New Zealand), low glucose Dulbecco's Modified Eagle's Medium (DMEM), DMEM/F12 and Neruobasal medium powder from Invitrogen Corporation (USA). Protein extraction kit and Bradford protein assay kit were purchased from Beijing SBS Genetech (China). Primary antibody Rabbit anti-NSE, Rabbit anti-GFAP, second antibody goat anti-Rabbit Cy3-IgG, HRP goat anti-rabbit IgG and DAB chromogenic detection kit were purchased from Wuhan Boster Biological Technology Co. Ltd. (China). The blocking solution was purchased from Beyotime Institute of Biotechnology (China) and used as it was. Primary antibody anti-connexin 36 rabbit polyclonal antibody, anti-pERK2 rabbit polyclonal antibody and anti-glyceraldehyde-3-phosphate dehydrogenase (GAPDH) rabbit polyclonal antibody were from Santa Cruz Biotechnology, Inc. (USA). Real time RT-PCR primers and the fluorogenic probe were purchased from Shanghai Xinghan Biotechnology Co. Ltd. (China). All other chemicals with analytical purity were purchased from Guangdong Guanghua Chemicals Co. Ltd. (China).

2.2. Neuroglial and neuron cell isolation and in vitro cultivation

BABL/c mice (0–3 days old) were sacrificed, the brain removed, and rinsed with dissection buffer to remove blood. Minced pieces of cortical gray matter were digested with 0.25% trypsinase and centrifuged for 5 min at 300 g at 4 °C. The pellet was resuspended in Dulbecco's Modified Eagle's Medium (DMEM) supplemented with 20% fetal bovine serum (FBS) and 1% penicillin–streptomycin. Cells were seeded into 50 ml polystyrene tissue culture flasks and allowed to adhere for 24 h. The cells were then incubated in a CO_2 incubator (5% CO_2, 95% air) (Thermo electron corporation, USA) at 37 °C and the medium was changed every four days. Glial fibrillary acidic protein staining was used to identify neuroglial cells. After the cells reached confluency, 2 ml of DMEM containing 0.25% trypsinase was added to the culture flask to create a cell suspension. The effect of 3-HB and derivatives (3-hydroxybutyrate methyl ester, 3-HBME, came from the methanolysis of polyhydroxybutyrate, and 3-hydroxybutyrate ethyl ester, 3-HBEE, came from the ethanolysis of polyhydroxybutyrate) on cell metabolic activity was determined for cultures seeded with 5×10^3 cells per well into 96 well plastic plates.

Dissociated hippocampal neurons were prepared from postnatal 0–3 day BABL/c mice by digestion of hippocampal tissue with 0.125% (w/v) trypsin for 10 min. DMEM/F12 medium containing 10% FBS was added, and three mild trituration and centrifugation steps were performed prior to resuspension in DMEM/F12 medium containing 10% FBS. The cells were seeded at 5×10^6 cells per well into glass bottom dishes coated with poly-L-lysine and incubated for 12 h to allow cells to adhere. Cytarabine was then added to a final concentration of 2.5 μg/ml to prevent glial cell proliferation, and after 24 h cells were cultured in neurobasal medium with 2% B27 and 1% Gln, with half the medium changed every 3 days. Immunostaining with neuron-specific enolase was used to identify neuronal cells.

2.3. 3-(4,5-Dimethylthiazol-2-yl)-2,5-diphenyl tetrazolium bromide (MTT) assay

The metabolic activity of neuroglial cells was evaluated by a MTT assay [21]. MTT was prepared as a 5 mg/ml stock solution in phosphate-buffered saline (0.1 M NaCl, 0.01 M Na_2PO_4, pH 7.2). To each well, 0.02 ml of MTT was added, and plates were incubated at 37 °C. After 4 h, the medium was removed, 0.1 ml dimethyl sulfoxide was added to each well, and the plates were gently rotated for 10 min to dissolve formazan. Six samples were prepared for each time point. The absorbance of samples at 570 nm was measured using an ELISA microplate reader (Bio-Rad model 550, USA). Control experiments indicated that 3-HB and derivatives did not stimulate cellular formazan production.

2.4. Fluorescence redistribution after photobleaching (FRAP) analysis of intercellular communication

Imaging and FRAP were performed using a Zeiss LSM 510 meta laser scanning confocal microscope (Germany) equipped with an argon laser source at 488 nm. Prior to microscopy, neurons were treated with 3-HBME, cells were rinsed with Hank's Buffered Salt Solution (HBSS), and loaded with 10 μg/ml 6-carboxyfluorescein diacetate (6-CFDA) at 37 °C in the presence of 5% CO_2 for 10 min. Cells were then rinsed with HBSS and observed in fresh culture medium without FBS. The CFDA fluorescence in a single cell soma was photobleached using a 488 nm laser, and fluorescence recovery in the photobleached compartment was then monitored for 620 s. For every photobleaching treatment, the entire soma of a single neuron was bleached and the fluorescence recovery was measured. All data represent the average ± SEM fluorescence recovery of six cells and are representative of three different FRAP experiments.

2.5. Morris water maze

Upon arrival, mice were allowed seven days to recover from transport before treatment. Mice were kept in standard rearing cages (30 × 20 × 14 cm) within an air-conditioned room (24 ± 1 °C) with a 12:12 h light:dark cycle. Food and water were supplied ad libitum. Sixty-two-month-old BALB/c mice were divided into five groups, each containing six males and six females: Negative control (treated with deionized water), 30 mg/kg/d acetyl-L-carnitine, 20 mg/kg/d 3-HBME, 30 mg/kg/d 3-HBME, and 40 mg/kg/d 3-HBME, each dissolved using deionized water as the solvent. Acetyl-L-carnitine improves rodents' performance in the Morris water maze and served as a positive control [22,23]. Mice were treated once daily through intragastric gavage for one month prior to the Morris water maze experiment.

The Morris water maze (Shanghai Jiliang Software Technology Co. Ltd., China) consisted of a circular pool (diameter 120 cm; height 60 cm) with black bottom and wall and water heated to 24 ± 1 °C. A black circular platform (diameter 6 cm; height 30 cm) was submerged 1 cm beneath the surface of the water. Because the color of the water tank including the pool bottom and the pool wall as well as the platform were black, the position of the platform was sufficiently obscured from the mice when the platform was submerged 1 cm beneath the surface of the water. On each of the walls of the four quadrants, a distinct colored paper was pasted as a visual positional cue. Four 45 W daylight lamps were positioned on the floor in the four corners of the arena and aimed at the ceiling to indirectly illuminate the surface of the water. A closed-circuit television camera was mounted onto the ceiling directly above the centre of the pool to monitor subject-swimming parameters.

2.5.1. Hidden platform test

All testing began at 09:30. During four daily acquisition sessions, each mouse was placed in the water facing the wall of the tank at one of the four designated starting points and allowed to swim and find the hidden platform located in the SW quadrant of the maze. During each trial, a mouse was given 60 s to find the hidden platform. If still in the water after 60 s, a mouse was gently guided to and placed on the platform. 10 s after climbing onto the platform, the mouse was placed on the next starting point. Swim paths and other data were recorded using a video camera connected to a tracking analysis system. The time the mouse required to reach the platform (escape latency), the total distance swam for each trial, and the swimming path in the pool was recorded.

2.5.2. Probe test

On the sixth day, the platform was removed from the pool and mice were challenged to a single search trial for 60 s (probe test). Four starting positions in the hidden platform were used for all mice. For the probe test, three parameters were measured, including the number of crossings of the exact place where the platform had been located, the swimming distance in the quadrant of the former platform position, and the swimming path in the pool.

2.5.3. Retention test

The retention test was conducted two days after the probe test and consisted of three trials from unique starting positions. After mounting the platform, mice were immediately placed in the holding cage for 40 s until the next trial.

2.5.4. Thigmotaxis

Thigmotactic swimming is defined as the behavior that mice display when swimming close to the walls of the water maze. The maze was divided into three circles of equal area, and the time spent in the outer ring of the pool was designated as "thigmotactic swimming" [24]. Thigmotaxis was reported as the percent of the total swimming time.

2.6. Western blot analysis

Total protein in hippocampal, subthalamic nucleus, frontal cortex, and temporal cortex tissue of mice was extracted using a protein extraction kit containing PMSF, EDTA, pepstatinA, leupeptin and aprotinin. Protein was measured by a Bradford protein assay kit.

After electrophoresis on 10% SDS-PAGE and electrotransfer, membranes were incubated in blocking solution on a rocker platform for 60 min at room temperature. Membranes were then incubated with primary antibody (either anti-connexin 36 rabbit polyclonal antibody, 1:400; anti-pERK2 rabbit polyclonal antibody, 1:100; or anti-glyceraldehyde-3-phosphate dehydrogenase (GAPDH) rabbit polyclonal antibody, 1:100) diluted in blocking solution on a rocker plate for 1 h at room temperature or overnight at 4 °C, washed three times for 10 min each in wash solution, incubated with HRP goat anti-rabbit IgG conjugate in blocking solution for 60 min on a rocker plate at room temperature, and washed three times for 10 min each in wash solution. The membranes were rinsed for 10 s in substrate buffer to remove residual detergent. Bands were visualized using a DAB chromogenic detection kit following the manufacturer's instructions.

2.7. Real time RT-PCR analysis

Total RNA was extracted and purified from hippocampal, subthalamic nucleus, frontal cortex, and temporal cortex tissue of mice using the RNeasy Mini Kit (Promega, USA) following the manufacturer's instructions. RNA yield was quantified by spectrophotometric analysis with a Biophotometer 6131 (Eppendorf, Germany), and the integrity of the RNA was verified by formaldehyde agarose gel electrophoresis.

Complementary DNA (cDNA) was prepared by reverse transcription of 250 ng total RNA using Superscript II enzyme and oligo dT primer. The reaction for each sample (total volume of 25 μl) was done in triplicate using an Applied Biosystem 7300 (USA) using the following conditions: 50 °C for 2 min, 95 °C for 10 min, and 40 cycles of 95 °C for 15 s and 60 °C for 1 min. PUMA-G gene transcript expression was normalized to the housekeeping gene GAPDH (Expression $= 2^{-\Delta Ct}$; $\Delta Ct = Ct_{Target} - Ct_{GAPDH}$). The level of expression in the control was designated as 1, with the results expressed as the fold difference relative to the control. PCR primers and the fluorogenic probe were designed using Primer Express 2.0 software. The PUMA-G specific PCR primers were as follows: Mouse PUMA-G forward primer: 5′-ggcgtggtgcagtgagca-3′; Mouse PUMA-G reverse primers: 5′-ctgcaggactctgtcttctt-cagt-3′; Mouse PUMA-G probe: 5′-tttggttgcgaggtgcagccataga-3′. The GAPDH specific probe and PCR primers were as follows: Forward primer: 5′-tgtgtccgtcgtggatctga-3′, GAPDH reverse primer: 5′-cctgcttcaccaccttcttga-3′, GAPDH probe: 5′-ccgcctggagaaacctgccaagtatg-3′.

2.8. Statistical analysis

All results were expressed as mean ± standard error of the mean (SEM). Statistical analyses including one-way ANOVA, one-way ANOVA with repeated measurements, or two-way ANOVA, all with *post hoc* Bonferroni test, were performed using XLSTAT software version 2008.4.02 (Addinsoft USA, New York, NY). A $p < 0.05$ was considered as statistically significant.

3. Results

3.1. Neuroglial cell metabolic activity

We previously demonstrated that medium supplemented with 5–100 mg/l 3-HB stimulated metabolic activity of cultured murine fibroblast L929 cells, human umbilical vein endothelial cells, and rabbit chondrocytes [25]. We therefore determined whether 3-HB and derivatives would stimulate metabolic activity of neuroglial cells. Overall treatment comparisons by two-way ANOVA indicated a statistically significant difference ($p < 0.0001$) between the three groups on each day of treatment. Treatment comparisons by Bonferroni's test indicated that significant differences existed between the 3-HB and 3-HBEE groups on day 1 ($p = 0.0052$) and day 3 ($p = 0.0001$) but not on day 2 ($p = 0.7776$), and that significant differences existed between the 3-HB and 3-HBME groups on all three days ($p < 0.0001$). Over 1–3 days in culture, 3-HB stimulated neuroglial cell metabolic activity, with statistically significant differences observed versus the control group from 0.5 to 10 mg/l. For the same time period, 3-HBEE or 3-HBME also significantly stimulated neuroglial cell metabolic activity, with statistically significant differences observed versus the control group from 0.5 to 10 mg/l (Fig. 1). Maximal stimulation was observed after three days treatment with 5 mg/l 3-HBEE, and after two days treatment with 5 mg/l 3-HB or 3-HBME.

3.2. Gap junctional intercellular communication

The enhanced proliferation of cultured cells effected by 3-HB is due to the inhibition of cell death at high confluencies [25]; conditions for which gap junctional intercellular communication could significantly impact cell survival. We therefore investigated whether 3-HBME treatment promoted gap junctional intercellular communication in dissociated cultures of hippocampal neurons. In these experiments, a cell was photobleached and the fluorescence intensity over time was recorded as unbleached dye molecules redistributed to the target cell through cell junctions with neighboring cells that contained active label (Fig. 2A–F). 6 min after photobleaching, fluorescence recovery for cells treated with 50 mg/l 3-HBME for less than 3 h and more than 5 h did not differ significantly (all $p > 0.05$) from the control cells (Fig. 2G). Cells treated with 50 mg/l 3-HBME for 3–5 h recovered from 30 to 70% of the initial fluorescence ($p < 0.05$ versus the control cells), with the greatest recovery observed for cells treated with 50 mg/l 3-HBME for 4 h. Fluorescence recovery was not observed for cells co-treated with 50 mg/l 3-HBME and either actinomycin D or cycloheximide (Fig. 2H).

3.3. Expression of connexin 36 and pERK2 in hippocampus tissues

Gap junctional intercellular channels are formed from a multigene family of proteins termed connexins. We next assessed the expression of connexin 36, an isoform expressed by hippocampal neurons [26], following 3-HBME treatment for 30 days. As compared with control mice that received deionized water, connexin 36 expression was 30% greater in hippocampal extracts from mice treated with 30 mg/kg/d 3-HBME (Fig. 3A–B). We also determined if acetyl-L-carnitine, which improve rodents performance in the Morris water maze [22], increased connexin 36 expression. Connexin 36 expression increased by 12% in hippocampal extracts from mice treated with 30 mg/kg/d acetyl-L-carnitine. These differences were not statistically significant.

Connexin assembly is modified by phosphorylation [27] through a signaling pathway involving phosphorylated ERK2 (pERK2) [28]. To determine if a similar pathway is activated by 3-HBME, pERK2 levels were determined in hippocampal extracts from control mice and mice treated with 30 mg/kg/d 3-HBME or 30 mg/kg/d acetyl-L-carnitine, normalizing the relative protein density to GAPDH. Mice treated with 3-HBME had pERK2 levels nearly twice that of either the control or acetyl-L-carnitine group, but statistically significant differences of pERK2 expression were not observed between the 3-HBME and control groups, or the acetyl-L-carnitine and control groups (Fig. 3C–D).

3.4. Transcription of PUMA-G mRNA in brain tissues

PUMA-G (protein up-regulated in macrophages by IFN-γ) is a G-protein-coupled receptor expressed in adipose tissue for which 3-HB has been proposed to serve as the endogenous ligand [15]. By real time RT-PCR, we demonstrated that PUMA-G mRNA was present in discrete brain regions of mice, including the hippocampus, subthalamic nucleus, temporal cortex, and frontal cortex (Fig. 4A). In the hippocampus, PUMA-G transcription was enhanced in mice treated with 30 mg/kg/d 3-HBME compared with the control group ($p < 0.05$, Fig. 4B).

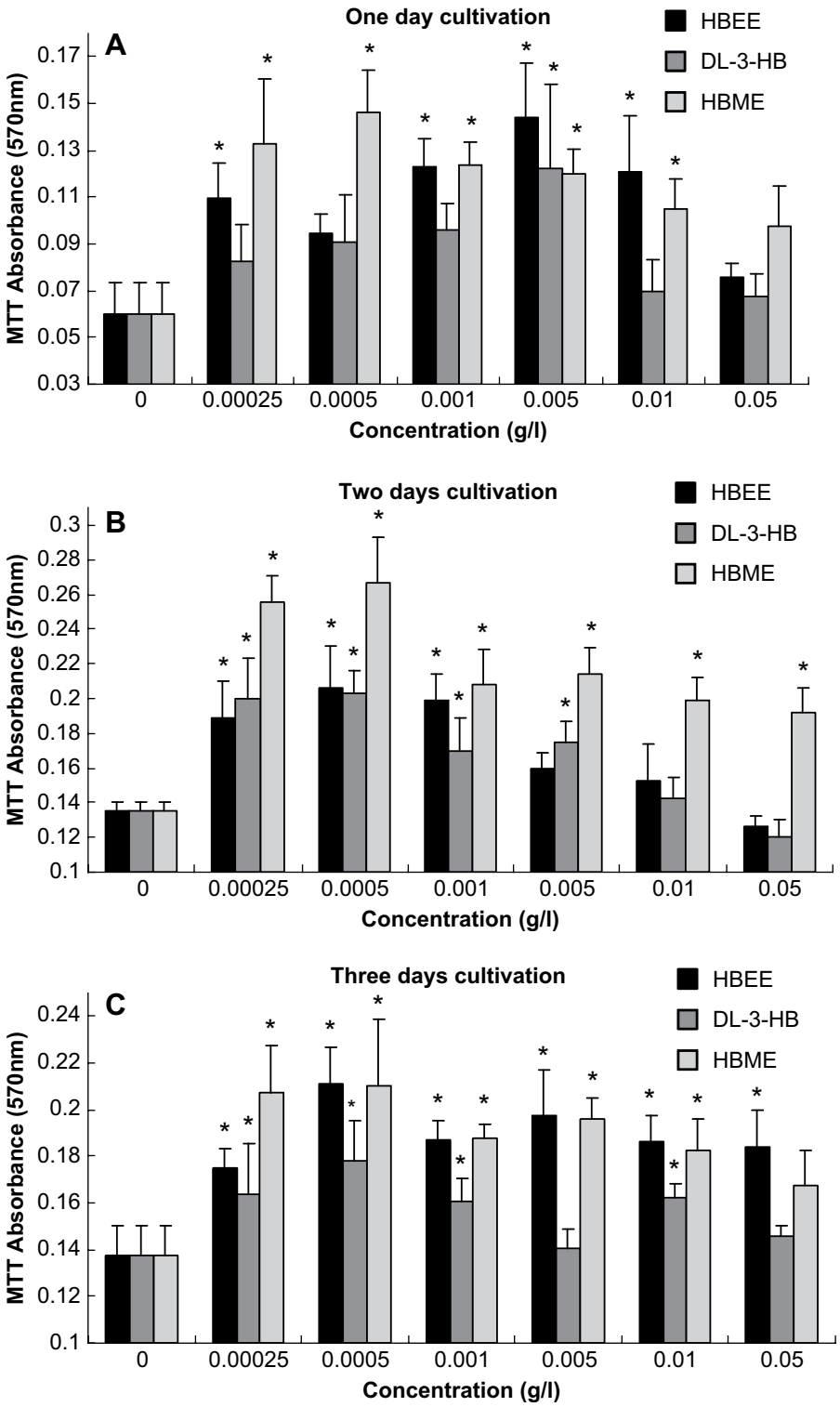

Fig. 1. 3-Hydroxybutyrate (3-HB) and derivatives stimulate metabolic activity of cultured mouse neuroglial cells. Plots are shown for cultures cultivated for (A) one day, (B) two days, (C) and three days in the presence of 3-HB, 3-hydroxybutyric acid ethyl ester (3-HBEE), and 3-hydroxybutyric acid methyl ester (3-HBME). Values represent the mean ± standard error of the mean ($n = 6$). Data were analyzed by two-way ANOVA, followed by Bonferroni post hoc analysis for multiple comparisons; $^{*}p < 0.05$.

3.5. Water maze learning

Gap junctions operate at the electrical synapse and mixed synapses containing both chemical and electrical synapses. As 3-HBME promoted gap junctional intercellular communication in cultured hippocampal neurons, we used the Morris water maze to assess whether 3-HBME influenced the ability of the mice to acquire, consolidate, and retain spatial information. One month prior to training, mice were treated with either 3-HBME (20, 30, or 40 mg/kg/d), 30 mg/kg/d acetyl-L-carnitine, or water. Compared with the control group, the food and water taken by all groups of mice did not differ during the one-month treatment prior to Morris

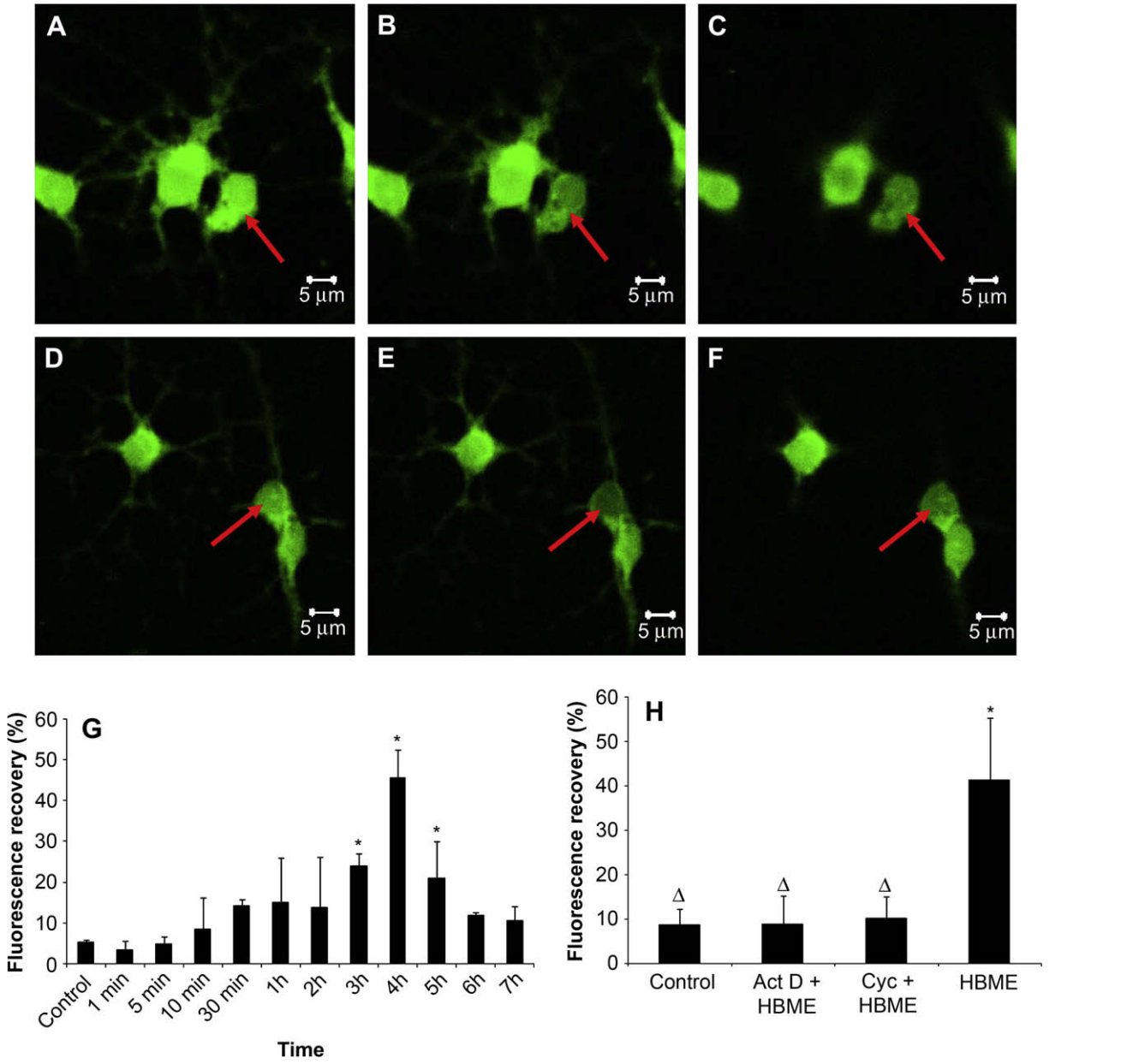

Fig. 2. 3-Hydroxybutyric acid methyl ester (3-HBME) transiently increases gap junctional intercellular communication between hippocampal neurons. Frames (A–C) show control neurons, whereas frames (D–F) show neurons treated with 50 mg/l 3-HBME for 5 h. (A,D) Fluorescence before photobleaching; (B,E) fluorescence immediately after photobleaching; (C,F) fluorescence 600 s after photobleaching; (G) fluorescence recovery 600 s after photobleaching versus treatment time with 50 mg/l 3-HBME ($n = 6$); (H) effect of actinomycin D (Act D) and cycloheximide (Cyc) on fluorescence recovery stimulated by 50 mg/l 3-HBME ($n = 6$). Error bars indicate the standard error of the mean. Data were analyzed by one-way ANOVA, followed by Bonferroni post hoc analysis for multiple comparisons; $^{*}p < 0.05$ versus control; $\Delta p < 0.05$ versus 3-HBME.

water maze experiments. After one month of treatment, the weight of mice treated with 30 and 40 mg/kg/d of 3-HBME increased by 52.57 ± 6.85, and $47.18 \pm 5.15\%$, respectively, differences that were statistically significant versus the control group ($38.93 \pm 3.33\%$), whereas the weight of mice treated with 20 mg/kg/d of 3-HBME and acetyl-L-carnitine increased by $39.90 \pm 5.58\%$ and $33.46 \pm 10.41\%$, respectively, differences that were not statistically significantly different compared with control group (Fig. 5A).

The escape latency of mice in all groups decreased with time. Overall treatment comparisons indicated that statistically significant differences existed among the groups. Notably, the 30 mM 3-HBME groups took less time ($p < 0.05$) than the control groups on days 1 and 3–5 to find the platform (Fig. 5B). All treatment groups were faster ($p < 0.05$) than the control group on day 5. Paths taken to the platform area on the fifth day of spatial training by mice in the 30 mg/kg/d 3-HBME group were more direct than those taken by mice in the control group, which took more circuitous paths (Fig. 5C). The total swimming distance of mice in all groups also decreased with time, and overall treatment comparisons indicated that a statistically significant difference existed for the groups. Similar to the escape latency results, the total swimming distance of the 30 mM 3-HBME groups was shorter ($p < 0.05$) than the control groups on days 1 and 3–5 (Fig. 5D). The total swimming distance for all treatment groups was shorter ($p < 0.05$) than the control groups at day 3–5, with the exception of the day 5 acetyl-L-carnitine group. Moreover, the total swimming distance of mice in the 30 mg/kg/d 3-HBME group was shorter ($p < 0.05$) than that of the control or other treatment groups at days 3–5.

A probe test was employed to determine how well the mice remembered the platform location [29]. Overall treatment

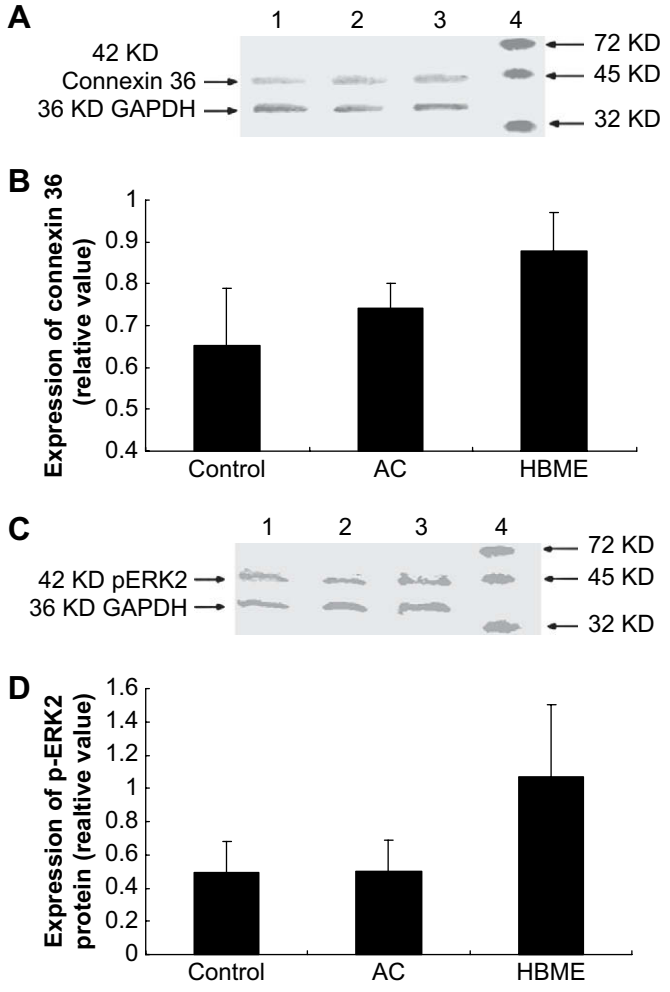

Fig. 3. Expression of connexin 36 and pERK2 protein levels in mouse hippocampal tissue. Mice were treated for 30 days with either deionized water, 30 mg/kg/d acetyl-L-carnitine (AC), or 30 mg/kg/d 3-hydroxybutyric acid methyl ester (3-HBME). (A) Western analysis; 42 kDa band, connexin 36; 36 kDa band, GAPDH; lane 1, control; lane 2, 30 mg/kg/d AC; lane 3, 30 mg/kg/d 3-HBME. (B) The relative protein density (relative value: protein density of connexin 36 protein/protein density of GAPDH protein) ± standard error of the mean ($n = 3$) are plotted. (C) Western blotting analysis; 42 kDa band, pERK2; 36 kDa band, GAPDH; lane 1, 30 mg/kg/d 3-HBME; lane 2, 30 mg/kg/d AC; lane 3, control. (D) The relative protein density (relative value: protein density of pERK2 protein/protein density of GAPDH protein) ± standard error of the mean ($n = 3$) are plotted.

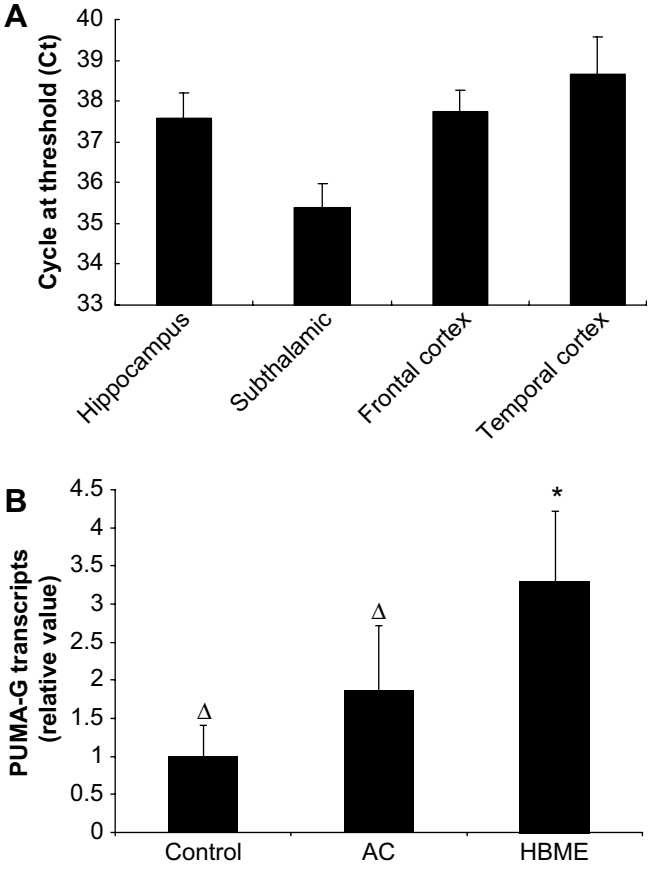

Fig. 4. PUMA-G mRNA is expressed in mouse brain. (A) PUMA-G expression in normal mice brain regions, as determined by real time RT-PCR. Values represent cycle threshold, error bars indicate the standard error of the mean ($n = 9$). (B) PUMA-G differational expression in hippocampus tissues. Mice were treated for 30 days with either deionized water, 30 mg/kg/d acetyl-L-carnitine (AC), or 30 mg/kg/d 3-hydroxybutyric acid methyl ester (3-HBME). PUMA-G gene transcript expressions were normalized by housekeeping gene GAPDH (Expression $= 2^{-\Delta Ct}$; $\Delta Ct = Ct_{Target} - Ct_{GAPDH}$). Expression levels in the control were designated as 1, whereas values following AC or 3-HBME treatment were expressed as the fold difference relative to the control. Error bars indicate the standard error of the mean ($n = 9$). Data were analyzed by one-way ANOVA, followed by Bonferroni post hoc analysis for multiple comparisons; $^{*}p < 0.05$; $\Delta p < 0.05$ versus 3-HBME.

comparisons for the number of times that mice crossed the former position of the hidden platform within 60 s indicated a statistically significant difference for the groups ($p = 0.0039$). Only the 30 mg/kg/d 3-HBME group was significantly different from the control (Fig. 5E). Overall treatment comparisons for the swimming distance in the quadrant of the former platform position indicated a significant difference among the groups ($p < 0.001$). All treatment groups were significantly greater versus the control group (Fig. 5F). The incidence of platform spans was greater ($p < 0.05$) for all groups versus the control group (Fig. 5G–H). The 3-HBME groups were similar to the acetyl-L-carnitine group. Overall treatment comparisons for the retention tests conducted two days after the probe test indicated a significant difference among the groups ($p = 0.0012$). All 3-HBME groups and the acetyl-L-carnitine group found the platform faster (all $p < 0.05$) than the control group (Fig. 5G–H). Overall treatment comparisons for the time spent near the maze walls, an indicator of thigmotaxis, indicated that a significant difference existed among the groups ($p < 0.001$). The degree of thigmotaxis decreased with training for all treated groups than did the controls, and for days 2–5 all 3-HBME groups and the acetyl-L-carnitine group spent less time ($p < 0.05$ for day 2, $p < 0.002$ for all groups on days 3–5) near the walls of the maze, on a percent basis, than did mice of the control group (Fig. 5I). In addition, the degree of thigmotaxis was lower in the 30 mg/kg/d 3-HBME group than in the acetyl-L-carnitine group ($p = 0.0018$).

4. Discussion

We examined the effect of hippocampal neuron and neuroglial cell treatment with 3-HB and derivatives on metabolic activity, macromolecular synthesis, and gap junctional intercellular communication, and on the performance of mice in the Morris water maze, toward the goal of elucidating the molecular mechanism by which 3-HBME improves the spatial learning ability of mice. Importantly, we demonstrated that PUMA-G, the endogenous receptor for 3-HB, is present in the hippocampus and upregulated in mice treated with 3-HBME. This treatment also activated gap junctional intercellular communication in hippocampal neurons. We will discuss how these findings provide an explanation for the underlying molecular mechanism of the stimulatory role of 3-HBME in learning and memory.

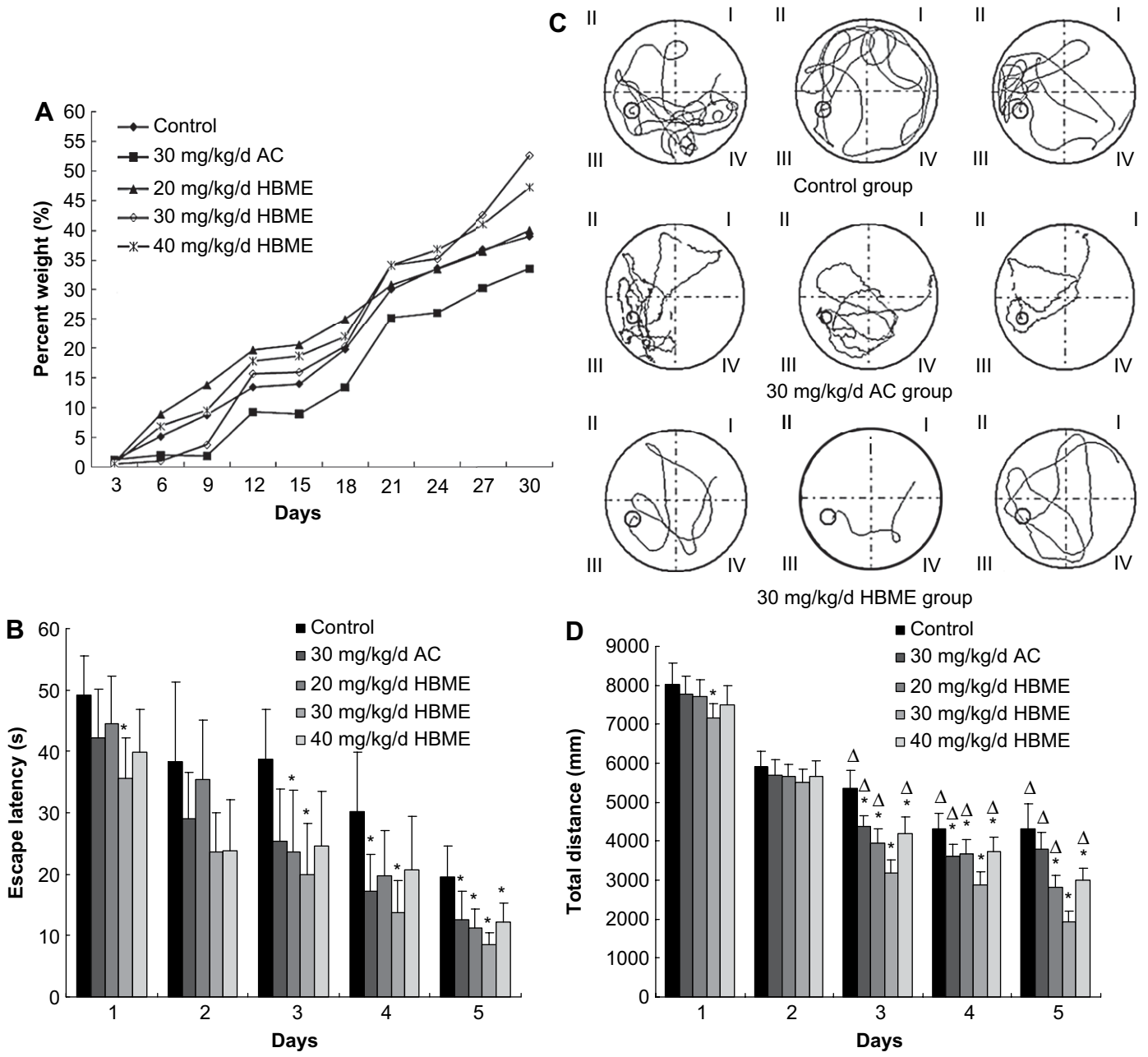

Fig. 5. Spatial learning and memory of mice was enhanced after treatment with acetyl-L-carnitine (AC) and 3-hydroxybutyric acid methyl ester (3-HBME). Mice were treated for 30 days with either deionized water, 30 mg/kg/d acetyl-L-carnitine, or 30 mg/kg/d 3-hydroxybutyric acid methyl ester. (A) Body weight versus treatment duration. (B) Escape latency. (C) Representative swimming paths. (D) The total swimming distance. (E) Platform spans in the probe test. (F) The swimming distance in the platform quadrant during the probe test. (G) Representative swimming paths during the probe test. (H) Retention tests. (I) Thigmotactic swimming behavior. Values represent the mean ± standard error of the mean ($n = 9$ or 10). Data were analyzed by one-way ANOVA with repeated measurements (B,D, and I) or one-way ANOVA (E,F, and H) followed by Bonferroni post hoc analysis for multiple comparisons; $^{*}p < 0.05$ versus control; $\Delta p < 0.05$ versus 30 mg/kg/d 3-HBME.

4.1. Stimulation of learning and memory by 3-HBME

After treatment for one month with 3-HBME or acetyl-L-carnitine, mice improved their memory acquisition skills, as judged by the hidden platform test. Mice in the 3-HBME and acetyl-L-carnitine groups also showed improved memory retention in the probe test. Collectively, these results suggest that 3-HBME enhanced learning and memory. During the probe trial, different search strategies were evident among the groups. Mice treated with 3-HBME went immediately to the target quadrant of the pool, demonstrating good analytical ability. In contrast, mice in the control group required more time to choose the target quadrant, first spending more time swimming near the periphery of the maze. This tendency to remain close to the walls, termed thigmotaxis, decreases gradually during the first minutes of exploration. The degree of thigmotaxis during this period is considered an index of anxiety in mice [30]. Based on this index, mice treated with 30 mg/kg/d 3-HBME seemed the calmest of the five groups. And although all four treatment groups displayed reduced escape latency versus the control, the swim distance for mice treated with 30 mg/kg/d 3-HBME was 500–1000 mm less than that of the other groups, and less than half that of the control group. Moreover, a dose response existed in the water maze behavior of mice treated with 3-HBME, such that those treated with 30 mg/kg/d responded better than those treated with 20 or 40 mg/kg/d. The mice treated with 20 mg/kg/d may have been under dosed, whereas the mice treated with 40 mg/kg/d may have

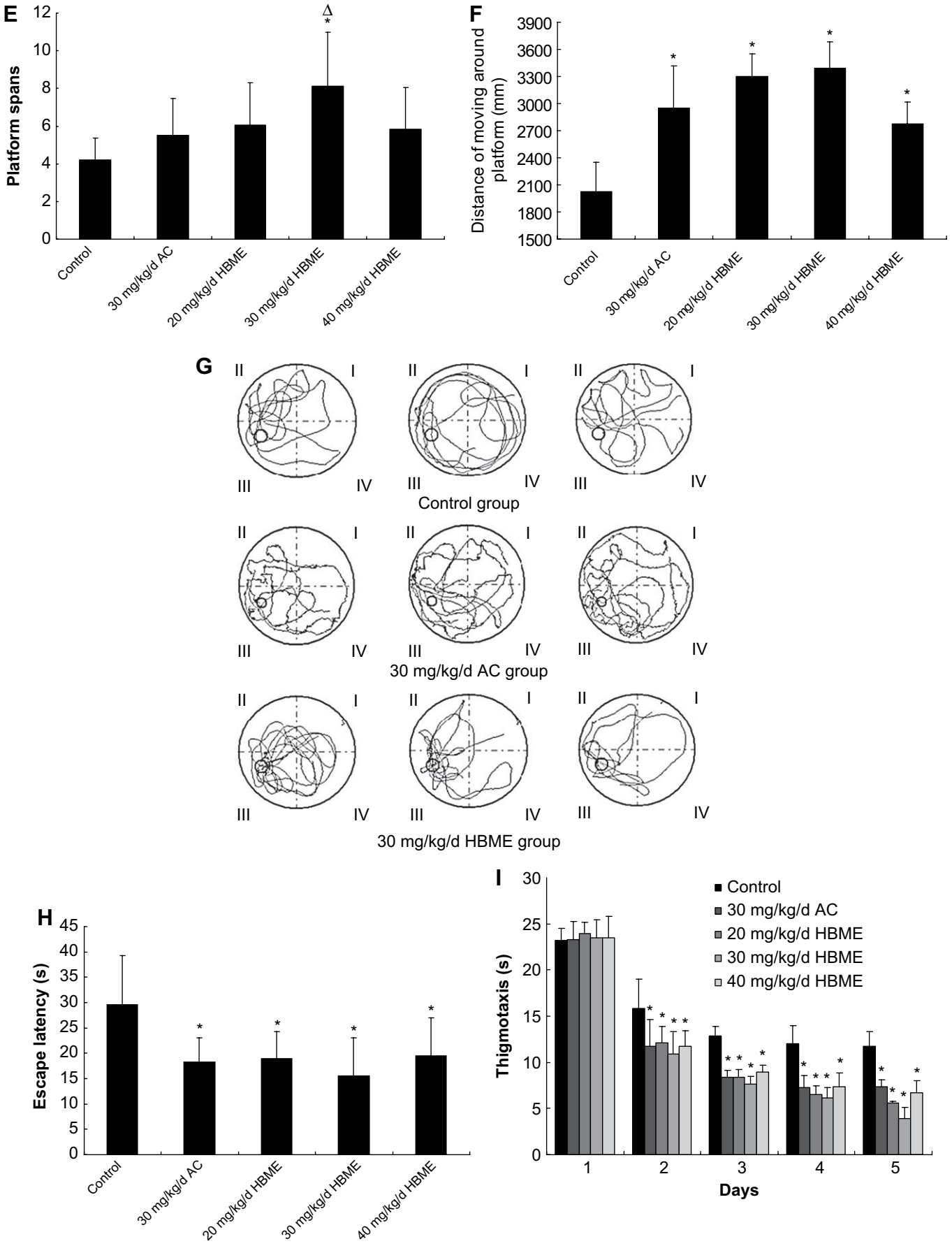

Fig. 5. (continued).

achieved plasma levels of 3-HBME that down-regulated the response. Evidence supporting such a dose response was obtained in experiments assessing the affects of 3-HBME on the metabolic activity of cultured cells. These possibilities require further testing. In summary, these results suggest that when mice treated with the 30 mg/kg/d dose of 3-HBME were first placed in the water; they remained calm, oriented themselves within the maze, and swam to the position where they expected to find the platform.

4.2. Gap junctional intercellular communication and neuroglial cell proliferative

Neuroglial cell metabolic activity was significantly promoted by 3-HB and derivatives, similar to the results of our previous study [25]. In that study, cell death of cultured murine fibroblast L929 cells was inhibited when 5–100 mg/l 3-HB was included in the medium. Although the explanation we put forth to explain this result, that 3-HB fuels mitochondria to maintain the $\Delta\psi_m$, remains plausible, the discovery that PUMA-G expression in brain is upregulated by 3-HBME led us to consider alternatives. A mechanism based on a signaling pathway mediated by a cell-surface receptor could account for the lack of affect at higher ($>$100 mg/l) 3-HB concentrations – cell-surface receptors can be inactivated or down-regulated. If 3-HB served to fuel mitochondria and augment ATP production, the proliferative effect would not appear bell shaped with respect to concentration. Furthermore, the affect of 3-HB on cell proliferation in our previous study was more apparent at high confluencies than at low confluencies. Cell-to-cell contacts would have a greater impact at high cell densities, as would gap junctional intercellular communication. Interestingly, connexin 36 knockout mice had impaired sensorimotor capacities and learning and memory processes, and displayed memory impairments that varied depending on the complexity of the stimuli presented, suggesting that neuronal gap junctions incorporating connexin 36 play a role in learning and memory [17].

Gap junctional intercellular communication between mammalian cells utilizes pores that allow for cytoplasmic continuity and the passage of molecules of less than 1 kDa in size. As these include cell messengers, ATP, and substrates of glycolysis and respiration, gap junctions help to maintain intracellular homeostasis across a population of contacting cells [31]. The necrotic death of an individual cell leads to the secondary cell death of its neighbors; therefore a cellular network in which weaker or stressed cells are supported by stronger cells is mutually beneficial. Curiously, tumor promoters block intercellular communication [32], and this block inhibits apoptosis [33], circumventing a safety checkpoint to safely remove cells malignant cells. We found increased expression of connexin 36 in mice hippocampus tissues, thus, 3-HBME may have applications to treat brain tumors, if these cells respond by upregulating gap junctional intercellular communication.

We observed a time-dependent increase in gap junctional intercellular communication between hippocampus neurons after treatment with 3-HBME. Fluorescence recovery was only observed for neurons treated with 3-HBME for 3–5 h, and was inhibited by actinomycin D and cycloheximide. No fluorescence recovery was observed for neurons treated for more than 6 h. This may result from PUMA-G down-regulation, as discussed in the following section. Specific physiological roles for gap junctional intercellular communication include response of tissues to hormones [34] and glial-guided neuronal migration [35]. In addition, under pathological circumstances, increased gap junctional intercellular communication might impair astrocytic control of the central nervous system microenvironment mediated by spatial buffering [36,37]. Our results support the possibility that 3-HBME treatment might also facilitate recovery after neuronal injury, or stabilize or promote the recovery of degenerating neurons.

4.3. PUMA-G expression in brain

In the brain, the storage and consolidation of new information involves molecular and structural modification of neurons [38,39], and long-term memory formation depends on protein synthesis [40,41]. Furthermore, systemic and central administrations of MAPK inhibitors reduce the reconsolidation of fear memory [42]. Along these lines, we observed increased levels of pERK2 in hippocampus that corresponded with an improved performance in the Morris water maze, which may reflect either an increased expression of total ERK2 protein, increased phosphorylation of ERK2, or a combination of both. Regardless, this indicates the involvement of signal pathways mediated by cell-surface receptors.

PUMA-G is a $G_{i/o}$-coupled seven-transmembrane receptor expressed in adipocytes and activated macrophages [43]. In mice, the fatty acid-derived ketone body 3-HB activates PUMA-G and inhibits mouse adipocyte lipolysis at concentrations observed in serum during fasting [15]. One report demonstrated expression of PUMA-G mRNA in lungs, spleen, heart, and skeletal muscle, whereas message level in kidney was low and not detectable in testis and brain [16]. Our results demonstrate that PUMA-G is expressed in brain tissues, including hippocampus, subthalamic nucleus, frontal cortex, and temporal cortex (Fig. 4A). Moreover, greater transcript levels were observed in the hippocampus following 3-HBME treatment compared with the control, suggesting that receptor activation upregulates expression. However, concentrations of 3-HB that were greater than 10 mg/l did not stimulate cell metabolic activity. Desensitization and down-regulation of PUMA-G may account for the bell shaped survival curve that we observed for 3-HB in this study.

Desensitization of G-protein-coupled receptors (GPCR) occurs by several distinct mechanisms. After agonist binding, a GPCR dissociates from G proteins, is rapidly phosphorylated, and then endocytosed. The receptor is eventually recycled to the cell surface or targeted for degradation. Down-regulation of the total number of cell-surface receptors after a prolonged treatment with an agonist is thought to mediate long-term desensitization. Interestingly, 3-HBME and 3-HBEE enhanced metabolic activity at higher concentrations than 3-HB. This may be due to prolonged receptor activation, with the esterified ligands affecting little desensitization. For another GPCR, the β2-adrenergic receptor, agonist stimulation stabilizes the dimeric state of the receptor, while inverse agonists favor the monomeric species [44]. Similarly, 3-HB may function as an inverse agonist and 3-HBME may function as an agonist of PUMA-G. Thus, the esterified ligands would have a wider functional concentration range in vivo. Finally, we note that some of the effects reported herein may be affected when 3-HB and derivatives bind the recently identified GHB receptor [45].

The precise mechanism by which 3-HBME enhances the acquisition of spatial memory is unknown. The discovery that 3-HBME upregulates PUMA-G and connexin 36 expression in the hippocampus suggests that gamma oscillations are a critical component in the formation of new synapses. Silent synapses, containing *N*-methyl-D-aspartate receptors, are highly plastic and may present a target for axons augmented with gap junctions [46]. Current from the gap junctions of electrical synapses would facilitate the induction of LTP [47]. Alternatively, 3-HBME could increase neuronal excitability to enhance the storage of new memories. Regardless, our data show that 3-HBME has potential applications to treat those cognitive disorders caused by synapse loss.

5. Conclusion

Our study showed clearly that PHB biodegradation product 3-HB and its derivative 3-HBME significantly improved the proliferation of neuroglial cells in vitro. Simultaneity, in FRAP, 3-HBME

enhanced GJIC of neurons. We first found that the transcript of PUMA-G in brain tissues of mice. After treating with 3-HBME, the enhanced transcript of PUMA-G and the increase of pERK2 protein had been detected. Importantly, in all MWM tests, we observed the best performance of mice in 30 mg/kg/d 3-HBME group, this result obvious showed that 3-HBME improved the learning and memory of mice.

Acknowledgements

We thank Zheming Zhou and Haibing Cui for performing intragastric gavage and Morris water maze experiments, Linping Wu for providing 3-HBME, and Xingnuan Li for neuroglial cell isolation and in vitro cultivation. This work was supported by the Li Ka Shing Foundation and Doctoral Initiating Project of Hanshan Normal University. The National High Tech 863 Grant (Project no. 2006AA02Z242) supported the PHA production project. Also, GQC was supported by 973 Basic Research Fund (Grant No. 2007CB707804) and Guangdong Provincial Grant for collaboration among industry, university and research organization.

Appendix

Figures with essential color discrimination. Fig. 2 in this article is difficult to interpret in black and white. The full color images can be found in the online version, at doi:10.1016/j.biomaterials.2008.12.012.

References

[1] Bontempi B, Laurent-Demir C, Destrade C, Jaffard R. Time-dependent reorganization of brain circuitry underlying long-term memory storage. Nature 1999;400:671–5.
[2] Thiagarajan TC, Lindskog M, Tsien RW. Adaptation to synaptic inactivity in hippocampal neurons. Neuron 2005;47:725–37.
[3] Wenk MR, De Camilli P. Protein–lipid interactions and phosphoinositide metabolism in membrane traffic: insights from vesicle recycling in nerve terminals. Proc Natl Acad Sci U S A 2004;101:8262–9.
[4] Bodles AM, Barger SW. Secreted beta-amyloid precursor protein activates microglia via JNK and p38-MAPK. Neurobiol Aging 2005;26:9–16.
[5] Morgan JR, Di Paolo G, Werner H, Shchedrina VA, Pypaert M, Pieribone VA, et al. A role for talin in presynaptic function. J Cell Biol 2004;167:43–50.
[6] Massieu L, Haces ML, Montiel T, Hernandez-Fonseca K. Acetoacetate protects hippocampal neurons against glutamate-mediated neuronal damage during glycolysis inhibition. Neuroscience 2003;120:365–78.
[7] Chen GQ, Wu Q. The application of polyhydroxyalkanoates as tissue engineering materials. Biomaterials 2005;26:6565–78.
[8] Kashiwaya Y, Takeshima T, Mori N, Nakashima K, Clarke K, Veech RL. D-beta-Hydroxybutyrate protects neurons in models of Alzheimer's and Parkinson's disease. Proc Natl Acad Sci U S A 2000;97:5440–4.
[9] Chung HJ, Steinberg JP, Huganir RL, Linden DJ. Requirement of AMPA receptor GluR2 phosphorylation for cerebellar long-term depression. Science 2003;300:1751–5.
[10] Kordower JH, Chu Y, Hauser RA, Freeman TB, Olanow CW. Lewy body-like pathology in long-term embryonic nigral transplants in Parkinson's disease. Nat Med 2008;14:504–6.
[11] Chu Y, Le W, Kompoliti K, Jankovic J, Mufson EJ, Kordower JH. Nurr1 in Parkinson's disease and related disorders. J Comp Neurol 2006;494:495–514.
[12] Kordower JH, Olanow CW. Regulatable promoters and gene therapy for Parkinson's disease: is the only thing to fear, fear itself? Exp Neurol 2008;209:34–40.
[13] Kompoliti K, Chu Y, Shannon KM, Kordower JH. Neuropathological study 16 years after autologous adrenal medullary transplantation in a Parkinson's disease patient. Mov Disord 2007;22:1630–3.
[14] Cheng S, Wu Q, Yang F, Xu M, Leski M, Chen GQ. Influence of DL-beta-hydroxybutyric acid on cell proliferation and calcium influx. Biomacromolecules 2005;6:593–7.
[15] Taggart AKP, Kero J, Gan X, Cai TQ, Cheng K, Ippolito M, et al. (D)-{beta}-Hydroxybutyrate Inhibits adipocyte lipolysis via the nicotinic acid receptor PUMA-G. J Biol Chem 2005;280:26649–52.
[16] Wise A, Foord SM, Fraser NJ, Barnes AA, Elshourbagy N, Eilert M, et al. Molecular identification of high and low affinity receptors for nicotinic acid. J Biol Chem 2003;278:9869–74.
[17] Frisch C, De Souza-Silva MA, Söhl G, Güldenagel M, Willecke K, Huston JP, et al. Stimulus complexity dependent memory impairment and changes in motor performance after deletion of the neuronal gap junction protein connexin36 in mice. Behav Brain Res 2005;157:177–85.
[18] Valappil SP, Misra SK, Boccaccini AR, Roy I. Biomedical applications of polyhydroxyalkanoates: an overview of animal testing and in vivo responses. Expert Rev Med Devices 2006;3:853–68.
[19] Ji Y, Li XT, Chen GQ. Interactions between a poly(3-hydroxybutyrate-*co*-3-hydroxyvalerate-*co*-3-hydroxyhexanoate) terpolyester and human keratinocytes. Biomaterials 2008;29:3807–14.
[20] Li XT, Zhang Y, Chen GQ. Nanofibrous polyhydroxyalkanoate matrices as cell growth supporting materials. Biomaterials 2008;29:3720–8.
[21] Denizot F, Lang R. Rapid colorimetric assay for cell growth and survival. Modifications to the tetrazolium dye procedure giving improved sensitivity and reliability. J Immunol Methods 1986;89:271–7.
[22] Liu JK, Head E, Gharib AM, Yuan W, Ingersoll RT, Hagen TM, et al. Memory loss in old rats is associated with brain mitochondrial decay and RNA/DNA oxidation: partial reversal by feeding acetyl-L-carnitine and/or R-alpha-lipoic acid. Proc Natl Acad Sci U S A 2002;99:2356–61.
[23] Chiechio S, Copani A, Gereau 4th RW, Nicoletti F. Acetyl-L-carnitine in neuropathic pain: experimental data. CNS Drugs 2007;21(Suppl. 1):31–8.
[24] Gass P, Wolfer DP, Balschun D, Rudolph D, Frey U, Lipp HP, et al. Deficits in memory tasks of mice with CREB mutations depend on gene dosage. Learn Mem 1998;5:274–88.
[25] Cheng S, Chen GQ, Leski M, Zou B, Wang Y, Wu Q. The effect of D,L-beta-hydroxybutyric acid on cell death and proliferation in L929 cells. Biomaterials 2006;27:3758–65.
[26] Rash JE, Yasumura T, Dudek FE, Nagy JI. Cell-specific expression of connexins and evidence of restricted gap junctional coupling between glial cells and between neurons. J Neurosci 2001;21:1983–2000.
[27] Lampe PD, Lau AF. Regulation of gap junctions by phosphorylation of connexins. Arch Biochem Biophys 2000;384:205–15.
[28] Ruch RJ, Trosko JE, Madhukar BV. Inhibition of connexin43 gap junctional intercellular communication by TPA requires ERK activation. J Cell Biochem 2001;83:163–9.
[29] Veng LM, Granholm AC, Rose GM. Age-related sex differences in spatial learning and basal forebrain cholinergic neurons in F344 rats. Physiol Behav 2003;80:27–36.
[30] Simon P, Dupuis R, Costentin J. Thigmotaxis as an index of anxiety in mice: influence of dopaminergic transmissions. Behav Brain Res 1994;61:59–64.
[31] Muriel A, Barberi-Heyob M, Stines JR, Blondel W, Dumas D, Guillemin F, et al. Gap junctional intercellular communication capacity by gap-FRAP technique: a comparative study. Biotechnol J 2007;2:50–61.
[32] Arenholt D, Philipsen HP, Nikai H, Andersen L, Jepsen A. Chemically unrelated tumor promoters induce identical morphological changes in cultured rat oral epithelium. Eur J Cancer Clin Oncol 1987;23:19–29.
[33] Sai K, Kang KS, Hirose A, Hasegawa R, Trosko JE, Inoue T. Inhibition of apoptosis by pentachlorophenol in v-myc-transfected rat liver epithelial cells: relation to down-regulation of gap junctional intercellular communication. Cancer Lett 2001;173:163–74.
[34] Murray SA, Fletcher WH. Hormone-induced intercellular signal transfer dissociates cyclic AMP-dependent protein kinase. J Cell Biol 1984;98:1710–9.
[35] Elias LAB, Wang DD, Kriegstein AR. Gap junction adhesion is necessary for radial migration in the neocortex. Nature 2007;448:901–7.
[36] Perez VJL, Frantseva MV, Naus CC. Gap junctions and neuronal injury: protectants or executioners? Neuroscientist 2003;9:5–9.
[37] Anders JJ. Lactic acid inhibition of gap junctional intercellular communication in in vitro astrocytes as measured by fluorescence recovery after laser photobleaching. Glia 1988;1:371–9.
[38] Abel T, Lattal KM. Molecular mechanisms of memory acquisition, consolidation and retrieval. Curr Opin Neurobiol 2001;11:180–7.
[39] Kompoliti K, Chu Y, Polish A, Roberts J, McKay H, Mufson EJ, et al. Effects of estrogen replacement therapy on cholinergic basal forebrain neurons and cortical cholinergic innervation in young and aged ovariectomized rhesus monkeys. J Comp Neurol 2004;472:193–207.
[40] Schafe GE, LeDoux JE. Memory consolidation of auditory pavlovian fear conditioning requires protein synthesis and protein kinase A in the amygdala. J Neurosci 2000;20:1–5.
[41] Coelln R, Thomas B, Andrabi SA, Lim KL, Savitt JM, Saffary R, et al. Inclusion body formation and neurodegeneration are parkin independent in a mouse model of alpha-synucleinopathy. J Neurosci 2006;26:3685–96.
[42] Atkins CM, Selcher JC, Petraitis JJ, Trzaskos JM, Sweatt JD. The MAPK cascade is required for mammalian associative learning. Nat Neurosci 1998;1:602–9.
[43] Tunaru S, Kero J, Schaub A, Wufka C, Blaukat A, Pfeffer K, et al. PUMA-G and HM74 are receptors for nicotinic acid and mediate its anti-lipolytic effect. Nat Med 2003;9:352–5.
[44] Hebert TE, Moffett S, Morello JP, Loisel TP, Bichet DG, Barret C, et al. A peptide derived from a beta2-adrenergic receptor transmembrane domain inhibits both receptor dimerization and activation. J Biol Chem 1996;271:16384–92.
[45] Andriamampandry C, Taleb O, Viry S, Muller C, Humbert JP, Gobaille S, et al. Cloning and characterization of a rat brain receptor that binds the endogenous neuromodulator gamma hydroxybutyrate (GHB). FASEB J 2003;17:1691–3.
[46] Hilbush BS, Morrison JH, Young WG, Sutcliffe JG, Bloom FE. New prospects and strategies for drug target discovery in neurodegenerative disorders. NeuroRx 2005;2:627–37.
[47] Bekinschtein P, Cammarota M, Katche C, Slipczuk L, Rossato JI, Goldin A, et al. BDNF is essential to promote persistence of long-term memory storage. Proc Natl Acad Sci U S A 2008;105:2711–6.